RSC Advances

PAPER

View Article Online
View Journal | View Issue

Cite this: *RSC Adv.*, 2020, **10**, 41883

SiC mesoporous membranes for sulfuric acid decomposition at high temperatures in the iodine–sulfur process†

Xin Yu, Qing Wang, Hiroki Nagasawa, Masakoto Kanezashi and Toshinori Tsuru *

Inorganic microporous materials have shown promise for the fabrication of membranes with chemical stability and resistance to high temperatures. Silicon-carbide (SiC) has been widely studied due to its outstanding mechanical stability under high temperatures and its resistance to corrosion and oxidation. This study is the first to prepare mesoporous SiC membranes for use in sulphuric acid decomposition to achieve thermochemical water splitting in the iodine–sulfur process. Single-gas permeation was carried out to confirm the stability of this mesoporous membrane under exposure to steam and H_2SO_4 vapor. Benefiting from the excellent chemical stability of the α-Al_2O_3 membrane support and the SiC particle layer, the SiC membrane exhibited stable gas permeance without significant degradation under H_2SO_4 vapor treatment at 600 °C. Additionally, with extraction, the membrane reactor exhibited an increased conversion from 25 to 41% for H_2SO_4 decomposition at 600 °C. The high performance combined with outstanding stability under acidic conditions suggests the developed SiC membrane is a promising candidate for H_2SO_4 decomposition in a catalytic membrane reactor.

Received 11th August 2020
Accepted 6th November 2020

DOI: 10.1039/d0ra06919a

rsc.li/rsc-advances

1. Introduction

Over the past twenty years, the water-splitting iodine–sulfur (IS) process has been extensively investigated as a sustainable technology with a net production of H_2 and O_2, at much lower temperatures compared with the direct thermal decomposition of water.[1–6] The IS process involves cyclic reactions such as the Bunsen reaction and the thermal decompositions of sulfuric acid at 850–950 °C and hydroiodic acid at 450 °C. In these cycles, the decomposition of sulfuric acid requires temperatures so high that the heat of solar or nuclear energy must be utilized.[3,5–7]

Net reaction:

$$2H_2O \leftrightarrow 2H_2 + O_2 \text{ (water-splitting)}$$

Bunsen reaction:

$$2H_2O + I_2 + SO_2 \leftrightarrow 2HI + H_2SO_4 \text{ (}\sim\text{120 °C)} \quad (1)$$

H_2 production:

$$2HI \leftrightarrow I_2 + H_2 \text{ (350–450 °C)} \quad (2)$$

O_2 production:

$$H_2SO_4 \leftrightarrow H_2O + SO_3 \text{ (}T > \text{300 °C)} \quad (3)$$

$$SO_3 \leftrightarrow SO_2 + 0.5O_2 \text{ (}\sim\text{850–950 °C)} \quad (4)$$

H_2SO_4 decomposes to produce O_2 in the following two steps: H_2SO_4 dissociates into H_2O at 300 °C (eqn (3)) and sulfur trioxide (SO_3), which further decomposes into sulfur dioxide (SO_2) and oxygen (eqn (4)) *via* catalysis around 850 to 950 °C. O_2 production from H_2SO_4 requires separation from co-produced SO_2, SO_3 and H_2O gaseous mixtures, while H_2 requires separation from HI and I_2. H_2 and O_2 are collected *via* the separation process for further applications. The high temperature of SO_3 decomposition (>850 °C) can be lowered *via* equilibrium shift by extracting O_2 from the reaction systems. Membrane-based separation methods such as microfiltration,[8] ultrafiltration,[9] nanofiltration,[10] reverse osmosis,[11] and gas separation[12] consume the least amount of energy compared with other separation techniques.[13] Membrane processes also provide a significant, convenient, and sustainable solution for H_2 and O_2 separation.[14–18]

In recent years, several types of membranes have been developed for the iodine–sulfur cycle.[4,19–28] Myagmarjav *et al.* reported that a hexyltrimethoxysilane (HTMOS) derived silica membrane achieved H_2 permeance on the order of 10^{-7} mol

Department of Chemical Engineering, Graduate School of Engineering, Hiroshima University, 1-4-1 Kagamiyama, Higashi-Hiroshima 739-8527, Japan. E-mail: tsuru@hiroshima-u.ac.jp

† Electronic supplementary information (ESI) available. See DOI: 10.1039/d0ra06919a

m^{-2} s^{-1} Pa^{-1} with H_2/HI selectivity of more than 175.[4] In addition, their silica-based ceramic membrane reactor achieved HI conversion of 0.70 and H_2 extraction of 0.98 at 400 °C.[27] However, it was also reported that silica membranes can't survive under humid environments at high temperatures,[29] and challenges remain for the use of silica membranes when using water in Bunsen reaction and H_2SO_4 decomposition reaction. Nomura *et al.* proposed a cation exchange membrane (CEM) constructed from polymerized divinylbenzene on Nafion for Bunsen reaction.[19] HI and H_2SO_4 were obtained separately from CEM-divided cells by feeding SO_2, I_2 and H_2O. He *et al.* discovered two Pt/carbon catalyst coated membranes (CCMs) that showed a reduced charge transfer resistance for the Bunsen reaction at room temperature.[24] The electrolytic voltage was reduced by 62.7% with cathode current efficiency that reached 97.41%. However, water permeated the cation exchange membrane to form H_2SO_4, and resistance to H_2SO_4 remains unsolved. Several recent results have also shown promising membrane performances under H_2SO_4 for the IS process. PTFE-based materials were reportedly stable even after exposure to highly concentrated H_2SO_4 solutions at 80–120 °C.[30] Non-fluorinated membranes (*e.g.*, polybenzimidazole, non-fluorinated poly(arylene ether sulfone)) have also shown excellent stability against 30 and 60 wt% H_2SO_4 at 80 °C.[31] However, for O_2 separation in integrated H_2SO_4 decomposition systems, stability under high temperatures (600–900 °C) for the second reaction, which is expressed as eqn (4), and for corrosion under strongly acidic conditions remains a challenge.

Generally, inorganic membranes are prepared with the strength to withstand high temperatures as well as oxidative and chemical conditions, which makes them promising candidates for O_2 separation from SO_3 decomposition, as mentioned in eqn (4). Notably, we reported several classes of inorganic membrane materials/metal oxides employed in membrane reactors for O_2/SO_3 separation.[3,5] SiO_2 membranes, due to their excellent thermal stability and high gas selectivity,[17,32] were first used by our team for O_2/SO_2 separation in 2015.[3] Bis(triethoxysilyl)ethane (BTESE)-derived membranes, particularly those fabricated under high temperatures, have demonstrated high oxidation resistance and exhibited an O_2/SO_3 selectivity of 10 with an O_2 permeance of 2.5×10^{-8} mol m^{-2} s^{-1} Pa^{-1}.[33] Despite a decrease in permeance after exposure to SO_3, the BTESE membrane exhibited a very high level of SO_3 stability. On the other hand, highly water stable BTESE membranes have also been studied,[17,34] and these have served as selective filters for $H_2O/O_2/SO_3$ separation. In addition, the membrane materials with high SO_3 (10% in O_2) resistance at 550 °C, such as SiO_2, SiO_2–ZrO_2 (high Si/Zr ratio), and α-Al_2O_3 powders were fundamentally studied.[5]

To the best of our knowledge, however, no study has yet reported the chemical stability of membrane materials against sulfuric acid at high temperatures (>400 °C), and as yet no effective strategy has been developed to fabricate an O_2-selective membrane structure. Moreover, there has been no report of an attempt to apply a membrane reactor to H_2SO_4 decomposition. However, the use of high temperatures is essential for the separation of O_2 though membrane and catalytic decomposition of H_2SO_4. The present study expands our previous work on the stability of various types of metal oxides under SO_3 exposure,[5] and provides insight from evaluating the characteristics of SiO_2, ZrO_2, SiC, homemade Al_2O_3, SiO_2–ZrO_2, and α-Al_2O_3 under H_2SO_4 vapor at high temperatures. After clarifying the chemical stability, the H_2SO_4 decomposition conversion of the membrane fabricated by SiC was further studied.

2. Experiments

2.1 Preparation of sol, gel and powders

SiO_2–ZrO_2 sols with sol concentrations of 2.0 wt% were synthesized from tetraethoxysilane (TEOS) and zirconium butoxide solutions (ZrBT, 80% in 1-butanol) in Si/Zr molar ratios of 5/5, 7/3 and 10/0 by hydrolysis and condensation reactions in H_2O with HCl (35 wt%) as the catalyst. The details can be found in our previous reports.[5,35] Al_2O_3 gels were prepared *via* hydrolysis and condensation by mixing aluminium tri-*sec*-butoxide (AlTBT, 97%) with water, and HCl in molar ratios of AlTBT/H_2O/HCl = 1/10/0.1. ZrO_2 sol was prepared *via* hydrolysis and condensation by mixing ZrBT, H_2O, and HCl in molar ratios of ZrBT/H_2O/HCl = 1/1/0.1. Ethanol (99.5%) was added to adjust the concentration of AlTBT or ZrBT sols at 5 wt%. Al_2O_3, SiO_2, ZrO_2, and SiO_2–ZrO_2 powders were prepared by drying Al_2O_3, SiO_2, ZrO_2, and SiO_2–ZrO_2 (Si/Zr ratio = 7/3) gels at 50 °C and subsequently calcined at 600 °C under air for 24 h.

2.2 Characterizations

After drying SiO_2, ZrO_2, homemade Al_2O_3, SiO_2–ZrO_2 (Si/Zr ratio of 7/3), and SiC powders at 600 °C under air, the exposure experiment was carried out in a quartz cell in which these powders were exposed to either H_2O or H_2SO_4 (98%) vapor under an absolute pressure of 1 bar at 600 °C for 24 h. Then, 2 ml of liquid (H_2O or H_2SO_4) was added into the quartz tube before heating, and after heating at 600 °C, and the vaporized liquid was refluxed in the tube as schematically shown in the diagram in the Fig. S1.† Powders were also exposed with an SO_3 of 10 kPa at 600 °C under sweep conditions similar to our previous report.[5] Subsequently, those powders were followed by drying at 500 °C under air to remove the adsorbed gas on the surface. Then, characterizations of powders were carried out using Energy Dispersive X-ray Spectroscopy (EDS) Scanning Electron Microscopy (SEM, JCM-5700, JEOL Ltd.), X-ray diffraction (XRD, Bruker AXS, Japan), and N_2 adsorption under liquid nitrogen at 77 K (BELMAX, BEL Japan Inc.).

2.3 Preparation of mesoporous membranes

Fabrication of membranes for H_2SO_4 separation, α-Al_2O_3 membrane support (cylindrical porous tubes with average pore size 2 μm; outer diameter 1 cm; length 10 cm, Nikkato. Corp.) were used as substrates. 5 types membranes were fabricated as shown in Table 1. The outer surfaces of the tube were coated with α-alumina (2.0 and 0.2 μm, Sumitomo Chemical Co., Ltd) or silicon carbide (2.3 and 0.5 μm, Pacific Rundum Co., Ltd.) particles mixed with the sols (SiO_2–ZrO_2 at Si/Zr ratio of 5/5, 7/3

Table 1 Conditions of the membrane fabrication by using various particles and binder sols

No.	Particles	Binder sols
M1	—	—
M2	α-Al_2O_3	SiO_2–ZrO_2 (5/5)
M3	α-Al_2O_3	SiO_2–ZrO_2 (7/3)
M4	SiC	SiO_2–ZrO_2 (7/3)
M5	SiC	SiO_2–ZrO_2 (10/0)

or 10/0) as the binder to create a smooth and homogeneous surface, followed by firing at 600 °C for 15 min then cooling to room temperature. This procedure of coating particle layers was repeated several times to reduce the pore sizes of the membranes to approximately 20 nm. The schematic membrane structure is shown in Fig. 1.

2.4 Gas permeance of membranes and H_2SO_4 conversion

The gas permeation of membranes during H_2SO_4 and H_2O exposure was tested in membrane module shown schematically in Fig. 2. Distilled H_2O (0.48 ml h^{-1}) or H_2SO_4 (1.0 ml h^{-1}) was introduced into the membrane *via* a syringe pump, and helium was supplied as a carrier gas (flow rate of 90 ml min^{-1}) to control the molar ratio of H_2O or H_2SO_4 at 0.1 bar. Membranes of different types, M1–M5, were placed in an electric furnace with a controlled inner-side temperature of 600 °C for evaporation and reaction. Once H_2SO_4 was injected inside the heated zone, liquid H_2SO_4 was evaporated, and then thermally decomposed into sulfur trioxide and water vapor. After exposure tests for several hours, membranes were dried with N_2 flow in the furnace at 600 °C, followed by cooling to room temperature. Then, the membrane module and gas lines were carefully cleaned by water to wash out the remaining H_2SO_4 and dried in an 80 °C oven. Pure gas permeance was measured under the transmembrane pressure difference from 0.01 to 1 bar by feeding gas to the outside of the membrane.

An M4 membrane was used for the membrane reactor to An M4 membrane was used for the membrane reactor to investigate the effect of O_2 extraction on H_2SO_4 decomposition conversion. At 600 °C, the liquid sulphuric acid changes to a gas phase, and the decomposition reaction can be split into two endothermic sub-reactions. The first sub-reaction is the dissociation of sulphuric acid into sulphur trioxide and water (reaction (3)), and the second is the decomposition of sulphur trioxide into sulphur dioxide and oxygen (reaction (4)). Here, SO_3 was decomposed to SO_2 with the Pt/Al_2O_3 catalyst (1.5 g, Shimadzu Corporation), which was packed inside the membrane. Outlet gases from the membrane reactor, consisting of mixtures of carrier gas He, and H_2O, SO_3, SO_2, and O_2, as produced from H_2SO_4 decomposition, subsequently passed through two bottles filled with 120 ml sodium hydroxide aqueous solution (20 wt%), where H_2O was condensed and SO_3 or SO_2 was trapped by the neutralization reaction. So the outlet gas consisted of He and O_2 and was measured using a soap film bubble flowmeter. NaOH was chosen for acidic gas absorption because it had high efficiency (nearly 100%) with SO_2 removal.[36] For safety, a SO_2 alarm (ToxiRAE II, PGM-1130) was set nearby the equipment to signal SO_2 leakage, and the outlet gas in the NaOH trap was monitored by the SO_2 alarm and the SO_2 content was found to be lower than 1 ppm.

H_2SO_4 conversion (w) can be quantified by the ratio of produced O_2 over theoretical O_2 since 1 mol of H_2SO_4 can produce 0.5 mol of O_2 after complete conversion. Therefore, the conversion can be expressed in the following equation:

$$w = \frac{F_r + F_p - F_c}{0.5F_h} \times 100\%$$

In that equation, F_r and F_p are the gas molar rate (mol s^{-1}) of retentate and permeate side of the membrane, F_c is the molar rate of carried gas He. F_h (mol s^{-1}) is the feed rate of liquid H_2SO_4. It is of note that H_2SO_4 was 100% decomposed to H_2O and SO_3 at 450 °C, hence, from this perspective, the H_2SO_4 conversion to SO_2 was dominated by SO_3 decomposition.

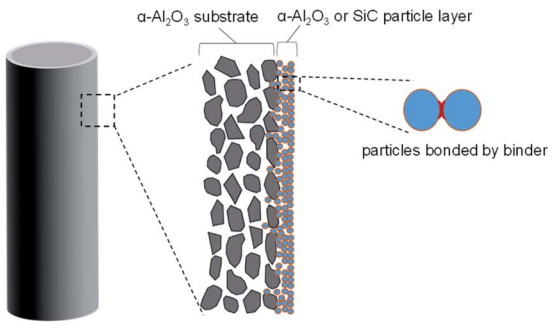

Fig. 1 The schematic structure of α-Al_2O_3 or SiC particle membranes.

3. Results and discussion

3.1 Stability of membrane materials under H_2SO_4 exposure

It has been pointed out that the α-Al_2O_3, SiO_2 and lower-Zr-content SiO_2–ZrO_2 powders had good chemical stability against SO_2 and SO_3 even at 550 °C for O_2/SO_2 or O_2/SO_3 separation.[5,37] The H_2SO_4 decomposition generates water vapor at temperatures higher than 300 °C, and, hence, the stability and corrosion under steam/acid still needs to be addressed. Therefore, Fig. 3 depicts the XRD patterns of the samples after being treated in SO_3 or H_2SO_4 vapor at 600 °C for 24 h. The XRD patterns of SiO_2 (Fig. 3A) showed a broad single peak centered at 23°, which was assigned to an amorphous SiO_2 phase, and no other peaks were observed in the XRD patterns. Additionally, Nadar *et al.* also reported that TG-DTA and XRD patterns of SiO_2 after H_2SO_4 exposure were similar to those before H_2SO_4,[38] indicating the high acid resistance of SiO_2. Table 2 shows the BET area of SiO_2 powders was largely decreased after being treated in steam and in H_2SO_4 vapor. The reason for this decrease in the BET area could have centered around the reaction of Si–O–Si and H_2O to form Si–OH, which could have led to large non-selective pores and resultant particles that became dense.[34,39] XRD analyses of α-Al_2O_3 (Fig. 3B) powders revealed that the S in $Al_2(SO_4)_3$ and the percentage of sulfur/aluminum

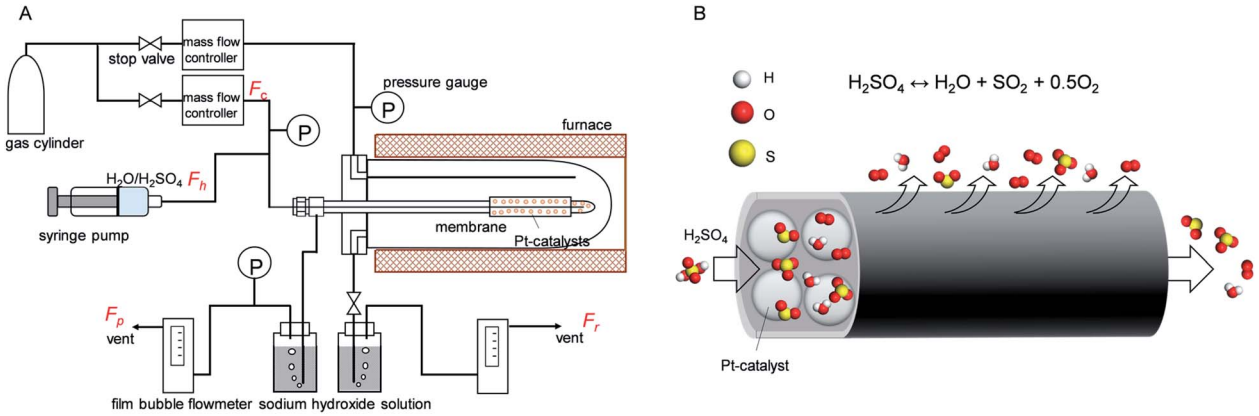

Fig. 2 (A) Schematic diagram of the experiment for steam and sulphuric acid treatment and gas permeance measurement. (B) Schematic illustration of the SiC membrane used membrane reactor for H_2SO_4 decomposition.

detected by EDS had increased from 0.87 to 26%, as shown in Table 2. Also, the FT-IR spectra confirmed that an SO_4 peak was formed in α-Al_2O_3 (ESI-2†), which was attributed to the reaction of alumina with the H_2SO_4 vapor at 600 °C. Furthermore, BET analyses revealed how the surface area of α-Al_2O_3 had decreased from 8.8 to 1.9 $m^2\ g^{-1}$ following exposure to H_2SO_4, presumably due to the formation of $Al_2(SO_4)_3$ on the surface, which reduced the size of the pores. Regarding the homemade Al_2O_3 powder, which had a high surface area of 226 $m^2\ g^{-1}$ compared with that of crystalline α-Al_2O_3 at 8.8 $m^2\ g^{-1}$, the BET area was drastically decreased after exposure to SO_3 and H_2SO_4, but the reactivity was significantly greater under H_2SO_4 vapor than under SO_3. Fig. 3C shows the XRD of ZrO_2, which exhibited an increased crystalline monoclinic (m) ZrO_2 from the tetragonal (t) phase[40] due to the temperature swings of the membrane furnace and the dryer oven. XRD analysis did not detect the sulfate phase for ZrO_2 and SiO_2–ZrO_2 (Si/Zr = 7/3) powders after SO_3 exposure, as shown in Fig. 3C and D, and corresponded to low S ratios of 2.7

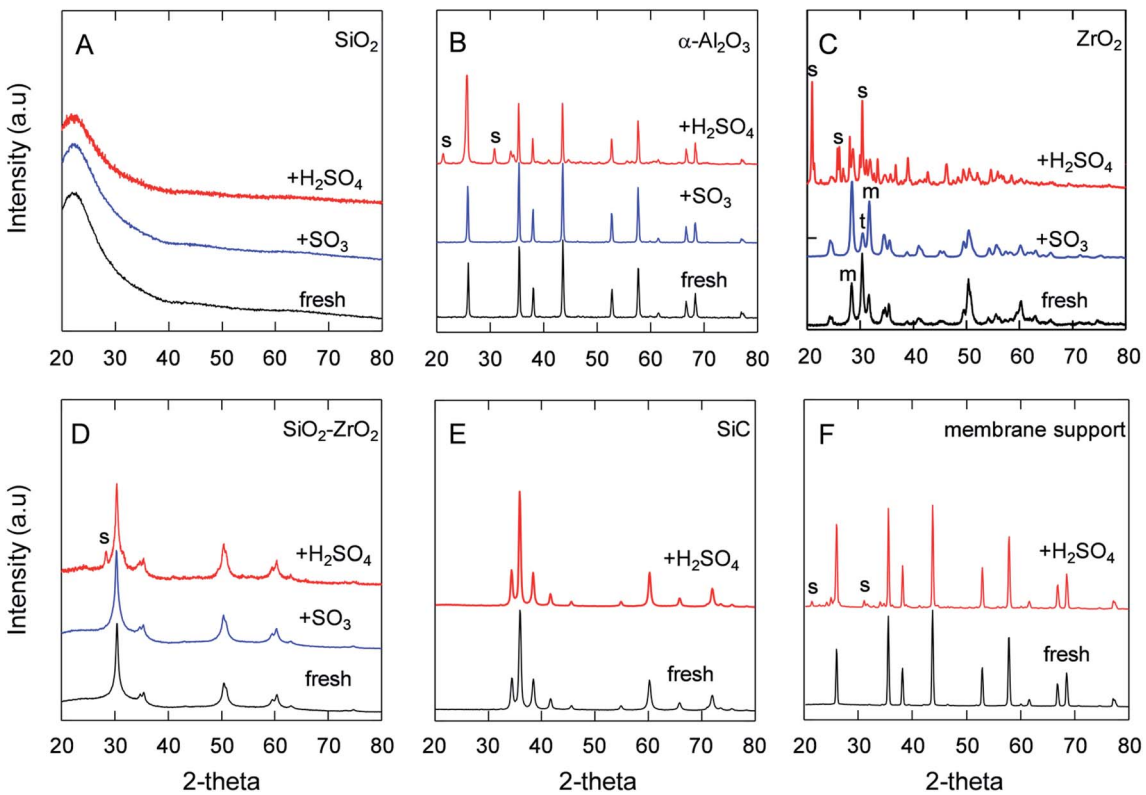

Fig. 3 XRD of different powders after SO_3 or H_2SO_4 exposure at 600 °C under one-atmosphere pressure. S: zirconium sulfate or aluminum sulfate, t/m: tetragonal/monoclinic ZrO_2. (A) Home-made SiO_2. (B) α-Al_2O_3. (C) ZrO_2. (D) SiO_2–ZrO_2 (Si/Zr = 7/3). (E) SiC. (F) α-Al_2O_3 membrane support.

Table 2 BET area and S ratio of powders after H_2O or H_2SO_4 exposure

Powders	Air-fired temperature (°C)	BET area (m^2 g^{-1})			S/Al or S/(Si + Zr) mole ratio (%)
		Fresh	After H_2O	After H_2SO_4	
SiO_2	600	650	600	390	<0.1
Home-made Al_2O_3	600	226	18	6.4	86
α-Al_2O_3	>1200	8.8	11	1.9	26
Membrane support	>1200	0.21	0.14	0.57	17
SiO_2–ZrO_2	600	115	25	14.9	4.0
ZrO_2	600	21	20	3.2	100
SiC	>1800	10.0	10.5	9.0	<0.1

and 2.2%,[5] respectively. On the contrary, after exposure to H_2SO_4 vapor at the same temperature of 600 °C, the S ratio was quite different between ZrO_2 and SiO_2–ZrO_2 powders. The XRD spectra in Fig. 3C shows the formation of $Zr(SO_4)_2$ from ZrO_2 after H_2SO_4 exposure, with only a small amount of crystalline $Zr(SO_4)_2$ (S peak)[41] detected for SiO_2–ZrO_2 (Fig. 3D). In addition, Table 2 shows the S content measured by EDS was almost 100 and 4.0% for ZrO_2 and SiO_2–ZrO_2 powders, respectively. Probable reasons for the high sulfur composition in ZrO_2 powders after exposure to H_2SO_4 vapor could be primarily that H_2O activated ZrO_2 and formed $ZrO(OH)_2$ or $Zr(OH)_4$ at high temperature.[42] Another explanation could be that either $ZrO(OH)_2$ or $Zr(OH)_4$ was more active in the reaction with SO_3 to form $Zr(SO_4)_2$. Fig. 3E shows the XRD spectra of silicon-carbide powders before and after H_2SO_4 exposure. No change in peaks was observed, probably because SiC is generally known for its ultrahigh chemical and thermal stability.[43–45] Additionally, the α-Al_2O_3 membrane supports used in this study were proven to be chemically stable under H_2SO_4, which was confirmed by XRD analysis to have a lesser amount of aluminum sulfate (Fig. 3F) compared with that of α-Al_2O_3 powders (Fig. 3B). This was probably because SiO_2 was added to the Al_2O_3 membrane supports since Si was detected in the Al_2O_3 membrane supports, although the exact content was not available. Although the S content was 17% for α-Al_2O_3 membrane supports after H_2SO_4 exposure, the change in the element composition of the substrates had less of an effect on gas permeation (Fig. 5). To benefit the stability of these materials against H_2SO_4 in the IS process, the use of α-Al_2O_3 membrane supports, SiC and SiO_2–ZrO_2 were proposed for the preparation of SiC membranes.

Fig. 4 features the SEM micrographs of SiO_2, α-Al_2O_3 and ZrO_2 before and after exposure to H_2SO_4. As shown in the images of Fig. 4A1 and A2, the surface of SiO_2 powders were smooth after H_2SO_4 exposure, which demonstrated morphological differences between the fresh state and after SO_3 exposure[5] while maintaining approximately the same particle size. This could be explained by the densification of SiO_2 fine particles induced by the reaction between Si–O–Si and H_2O. Fig. 4B1 and B2 shows that α-Al_2O_3 particles had a relatively uniform morphology even after H_2SO_4 exposure while the size of the Al_2O_3 particles grew larger due to the formation of low-melting $Al_2(SO_4)_3$ on the surface, with which each of the primary particles seemed to be connected and aggregated that differed from the α-Al_2O_3 particles with SO_3 exposure.[5] Given that α-Al_2O_3 particles after exposure were deposited with, and covered by, the $Al_2(SO_4)_3$, these SEM photos confirm the compositions obtained by EDS. The SEM images in Fig. 4C1 and C2 also show that the fine ZrO_2 particles had reacted with the H_2SO_4 vapor and increased in size, which is similar to the growth of α-Al_2O_3 powder under H_2SO_4 exposure, probably due to the effect of dissolution under the H_2O vapor and to the reaction with SO_3.

3.2 Permeance of the SiC membrane reactor for H_2SO_4 decomposition

Porous inorganic membranes were first explored under an extreme condition, *i.e.*, H_2SO_4 decomposition at 600 °C. Fig. 5

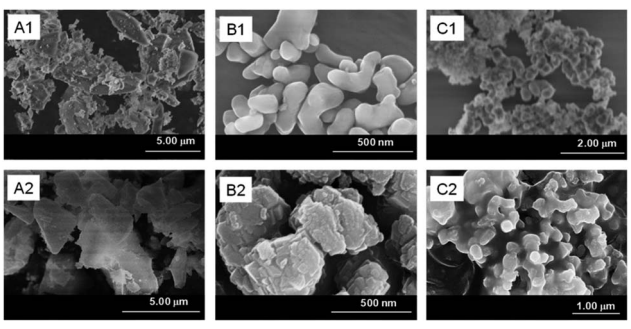

Fig. 4 SEM of fresh SiO_2 (A1), α-Al_2O_3 (B1), ZrO_2 (C1) powders. (A2), (B2) and (C2) were those powders after H_2SO_4 (100 kPa) exposure at 600 °C, respectively.

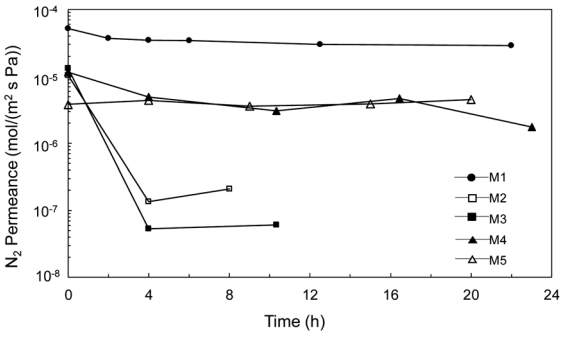

Fig. 5 Time course of N_2 permeance for α-Al_2O_3 membrane support (M1) and membrane prepared by Al_2O_3 particle layer (M2, M3), and SiC particle (M4, M5) after the treatment under H_2SO_4 vapor at 600 °C.

shows the time course of the N_2 permeance with increases in the treatment time under H_2SO_4 vapor. The N_2 permeance of the α-Al_2O_3 membrane support (M1) was decreased only slightly even after 22 h of exposure to H_2SO_4 vapor at 600 °C, since the membrane support provided only moderate chemical stability, as shown in Fig. 3F (XRD) and Table 2, and the large pores changed very little even after sulfate formation. M2, M3, and M4 prepared with different particles (SiC, α-Al_2O_3) and binders (SiO_2–ZrO_2, SiO_2) showed N_2 permeance at the same level (10^{-5} mol m^{-2} s^{-1} Pa^{-1}) as before the stability test, which provided a fair comparison and verified good reproducibility of the membrane fabrication. Values were drastically decreased for the permeance of both M2 and M3 Al_2O_3 particle layers following H_2SO_4 exposure for 4 h. The permeance of M2 was further decreased, however, confirming that the high Zr content in the binder (Si/Zr = 5/5) was more unstable due to the formation of $Zr(SO_4)_2$ with H_2SO_4, similar to high Zr content SiO_2–ZrO_2 (Si/Zr = 5/5) in SO_3.[5] These results were reasonable, and strongly suggested that the membranes should be prepared using Si-rich SiO_2–ZrO_2 (Si/Zr = 7/3) as a binder. M4 and M5 SiC particle layers showed a very small decrease and high relative permeance over all the particle membranes, M2–M5. That indicated that the membrane prepared by SiC with Si-rich SiO_2–ZrO_2 (Si/Zr = 7/3) increased both the chemical and hydrothermal stability compared with that of the Al_2O_3 particle layers with Zr-rich SiO_2–ZrO_2 used to fabricate M2 and M3. The morphology changed less for membranes fabricated with SiC layers following exposure to H_2SO_4 (ESI-3†), which corresponds to the stability confirmed by XRD and BET results. These results suggested that the SiC was stable for fabricating a particle layer for membrane preparation in the IS process.

Catalytic membrane reactor for H_2SO_4 decomposition, liquid H_2SO_4 (98%) was fed at a flow rate of 1.0 ml h^{-1} and He was used as the carrier gas with a flow rate of 24.5 ml min^{-1} controlled by a mass flow controller. Fig. 6 shows the time course for the total flow rate of the outlet gas in both the retentate and permeate, and the conversion of H_2SO_4 decomposition at 600 °C in a SiC particle-derived membrane reactor. A brief flow sheet with or without extraction is shown in ESI-4.† The membrane reactor with extraction, O_2 with low molecular weight was transferred faster than SO_2 and SO_3, and SO_3, and the largest molecular weight, permeated at the slowest speed by Knudsen diffusion through the mesoporous SiC membrane.[46] Therefore, the equilibrium of the reaction (R4) ($SO_3 \leftrightarrow SO_2 + 0.5O_2$) was forwarded to the product side by removing O_2. In a comparison with a membrane without extraction, the membrane reactor with extraction achieved higher conversion at the same temperature of 600 °C. The catalytic membrane reactor obtained conversion of 25% without extraction, which approximated the equilibrium (theoretical) conversion of SO_3 decomposition (eqn (4)) of 28% at 900 K.[3] Comparison with membrane without extraction, the conversion of H_2SO_4 decomposition was increased to 45%, which was much higher at the same temperature of 600 °C. Additionally, the H_2SO_4 decomposition conversion remained constant at around 41% after membrane exposure to H_2SO_4 vapor for 10 h. Moreover, after decomposition for 10 h, He permeance was approximately the same as that before the decomposition reaction, which indicated that the SiC particle layer (with SiO_2–ZrO_2) had high hydrothermal and chemical stability under H_2O and SO_3. However, the separation properties of M4 membranes was still poor; the He/N_2 permeance ratio was 2.3 with N_2 permeance of 4.5×10^{-5} mol m^{-2} s^{-1} Pa^{-1}, since the SiC membrane was fabricated using SiC particles, and the gaps between particles were large enough to allow gas to pass through.

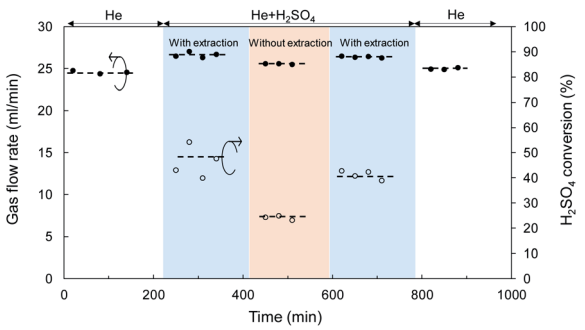

Fig. 6 Time course of gas flow rate and H_2SO_4 conversion for a SiC membrane tested in the catalytic membrane reactor at 600 °C.

4. Conclusions

SiC mesoporous membranes were successfully prepared using an α-Al_2O_3 support and a SiC particle layer. The gas permeance of the SiC membrane was stable for 20 h under H_2SO_4 vapor at 600 °C, which indicated its high chemical stability. Regarding the H_2SO_4 decomposition reaction, the SiC membrane achieved a conversion of 41% at 600 °C, which was much higher than that of the membrane without extraction (25%). Our previous work involved the preliminary use of SiC membranes in a catalytic membrane reactor for hydrogen production in the iodine–sulfur process, and a desirable design for a SiC subnanoporous membrane with a combination of high O_2 permeance and O_2/SO_2 selectivity will be a major objective in the future.

Conflicts of interest

There are no conflicts to declare.

Acknowledgements

This work was supported by the Cross-ministerial Strategic Innovation Promotion Program (SIP) of the Energy Carrier Project of the Japan Science and Technology Agency (JST) and the Japan Society for the Promotion of Science (JSPS) KAKENHI Grant Number JP20H052279.

Notes and references

1 S. Kasahara, G.-J. Hwang, H. Nakajima, H.-S. Choi, K. Onuki and M. Nomura, Effects of process parameters of the IS process on total thermal efficiency to produce hydrogen from water, *J. Chem. Eng. Jpn.*, 2003, **36**, 887–899.

2 D. M. Ginosar, H. W. Rollins, L. M. Petkovic, K. C. Burch and M. J. Rush, High-temperature sulfuric acid decomposition over complex metal oxide catalysts, *Int. J. Hydrogen Energy*, 2009, **34**, 4065–4073.

3 L. Meng, M. Kanezashi and T. Tsuru, Catalytic membrane reactors for SO_3 decomposition in iodine–sulfur thermochemical cycle: a simulation study, *Int. J. Hydrogen Energy*, 2015, **40**, 12687–12696.

4 O. Myagmarjav, A. Ikeda, N. Tanaka, S. Kubo and M. Nomura, Preparation of an H_2-permselective silica membrane for the separation of H_2 from the hydrogen iodide decomposition reaction in the iodine–sulfur process, *Int. J. Hydrogen Energy*, 2017, **42**, 6012–6023.

5 X. Yu, L. Meng, H. Nagasawa, M. Kanezashi, M. Machida and T. Tsuru, Evaluating the chemical stability of metal oxides in SO_3 and applications of SiO_2-based membranes to O_2/SO_3 separation, *J. Am. Ceram. Soc.*, 2019, **102**, 6946–6956.

6 A. Nadar, A. M. Banerjee, M. Pai, S. S. Meena, R. Pai, R. Tewari, S. Yusuf, A. Tripathi and S. Bharadwaj, Nanostructured Fe_2O_3 dispersed on SiO_2 as catalyst for high temperature sulfuric acid decomposition—structural and morphological modifications on catalytic use and relevance of Fe_2O_3-SiO_2 interactions, *Appl. Catal., B*, 2017, **217**, 154–168.

7 M. Nomura, Application of an electrochemical membrane reactor to the thermochemical water splitting IS process for hydrogen production, *J. Membr. Sci.*, 2004, **240**, 221–226.

8 X. Liu, B. Jiang, X. Yin, H. Ma and B. S. Hsiao, Highly permeable nanofibrous composite microfiltration membranes for removal of nanoparticles and heavy metal ions, *Sep. Purif. Technol.*, 2020, **233**, 115976.

9 P. H. Duong, V. A. Kuehl, B. Mastorovich, J. O. Hoberg, B. A. Parkinson and K. D. Li-Oakey, Carboxyl-functionalized covalent organic framework as a two-dimensional nanofiller for mixed-matrix ultrafiltration membranes, *J. Membr. Sci.*, 2019, **574**, 338–348.

10 S. Anisah, W. Puthai, M. Kanezashi, H. Nagasawa and T. Tsuru, Preparation, characterization, and evaluation of TiO_2-ZrO_2 nanofiltration membranes fired at different temperatures, *J. Membr. Sci.*, 2018, **564**, 691–699.

11 G. Dong, H. Nagasawa, L. Yu, M. Guo, M. Kanezashi, T. Yoshioka and T. Tsuru, Energy-efficient separation of organic liquids using organosilica membranes via a reverse osmosis route, *J. Membr. Sci.*, 2020, **597**, 117758.

12 Y. Ying, M. Tong, S. Ning, S. K. Ravi, S. B. Peh, S. C. Tan, S. J. Pennycook and D. Zhao, Ultrathin Two-Dimensional Membranes Assembled by Ionic Covalent Organic Nanosheets with Reduced Apertures for Gas Separation, *J. Am. Chem. Soc.*, 2020, **142**, 4472–4480.

13 C. Z. Liang, T.-S. Chung and J.-Y. Lai, A review of polymeric composite membranes for gas separation and energy production, *Prog. Polym. Sci.*, 2019, **97**, 101141.

14 L. Yu, M. Kanezashi, H. Nagasawa, N. Moriyama, T. Tsuru and K. Ito, Enhanced CO_2 separation performance for tertiary amine-silica membranes via thermally induced local liberation of CH_3Cl, *AIChE J.*, 2018, **64**, 1528–1539.

15 X. Ren, M. Kanezashi, H. Nagasawa and T. Tsuru, Plasma-assisted multi-layered coating towards improved gas permeation properties for organosilica membranes, *RSC Adv.*, 2015, **5**, 59837–59844.

16 G. Gong, H. Nagasawa, M. Kanezashi and T. Tsuru, Reverse osmosis performance of layered-hybrid membranes consisting of an organosilica separation layer on polymer supports, *J. Membr. Sci.*, 2015, **494**, 104–112.

17 T. Tsuru, Silica-Based Membranes with Molecular-Net-Sieving Properties: Development and Applications, *J. Chem. Eng. Jpn.*, 2018, **51**, 713–725.

18 M. Elimelech and W. A. Phillip, The future of seawater desalination: energy, technology, and the environment, *Science*, 2011, **333**, 712–717.

19 M. Nomura, T. Kodaira, A. Ikeda, Y. Naka, H. Nishijima, S.-i. Imabayashi, S.-i. Sawada, T. Yamaki, N. Tanaka and S. Kubo, Development of ion-exchange membranes for the membrane bunsen reaction in thermochemical hydrogen production by iodine-sulfur process, *J. Chem. Eng. Jpn.*, 2018, **51**, 726–731.

20 O. Myagmarjav, J. Iwatsuki, N. Tanaka, H. Noguchi, Y. Kamiji, I. Ioka, S. Kubo, M. Nomura, T. Yamaki and S. Sawada, Research and development on membrane IS process for hydrogen production using solar heat, *Int. J. Hydrogen Energy*, 2019, **44**, 19141–19152.

21 O. Myagmarjav, N. Tanaka, M. Nomura and S. Kubo, Module design of silica membrane reactor for hydrogen production via thermochemical IS process, *Int. J. Hydrogen Energy*, 2019, **44**, 10207–10217.

22 N. Tanaka, H. Noguchi, Y. Kamiji, H. Takegami and S. Kubo, Hydriodic iodide and iodine permeation characteristics of fluoropolymers as a lining material, *Int. J. Hydrogen Energy*, 2020, **45**, 17557–17561.

23 B. Bhushan, N. Goswami, S. Parida, B. Rath, S. A. Kumar, V. Karki, R. Bindal and S. Kar, Corrosion behavior analyses of metallic membranes in hydrogen iodide environment for iodine-sulfur thermochemical cycle of hydrogen production, *Int. J. Hydrogen Energy*, 2018, **43**, 10869–10877.

24 B. Huang, Y. Zhu, Y. He, S. Xu, Y. Zhang and Z. Wang, Influence of catalyst coated membranes on electrochemical bunsen reaction in the sulfur-iodine cycle, *Int. J. Hydrogen Energy*, 2019, **44**, 9735–9742.

25 C. Forsberg, L. Trowbridge, B. Bischoff and L. K. Mansur, Sulfur thermochemical processes with inorganic membranes to produce hydrogen, *Citeseer, AIChE Spring National Meeting New Orleans*, Louisiana, USA, 2004.

26 G. He, R. H. Elder, D. C. Sinclair and R. W. K. Allen, High temperature oxygen separation for the sulphur family of thermochemical cycles – Part II: sulphur poisoning and membrane performance recovery, *Int. J. Hydrogen Energy*, 2013, **38**, 785–794.

27 O. Myagmarjav, N. Tanaka, M. Nomura and S. Kubo, Comparison of experimental and simulation results on catalytic HI decomposition in a silica-based ceramic membrane reactor, *Int. J. Hydrogen Energy*, 2019, **44**, 30832–30839.

28 L. Meng, M. Kanezashi, X. Yu and T. Tsuru, Enhanced decomposition of sulfur trioxide in the water-splitting iodine–sulfur process via a catalytic membrane reactor, *J. Mater. Chem. A*, 2016, **4**, 15316–15319.

29 M. Elma, C. Yacou, J. C. Diniz da Costa and D. K. Wang, Performance and long term stability of mesoporous silica membranes for desalination, *Membranes*, 2013, **3**, 136–150.

30 G. Caputo, C. Felici, P. Tarquini, A. Giaconia and S. Sau, Membrane distillation of $HI/H_2OHI/H_2O$ and $H_2SO_4/H_2OH_2SO_4/H_2O$ mixtures for the sulfur–iodine thermochemical process, *Int. J. Hydrogen Energy*, 2007, **32**, 4736–4743.

31 H. Schoeman, H. M. Krieg, A. J. Kruger, A. Chromik, K. Krajinovic and J. Kerres, H_2SO_4 stability of PBI-blend membranes for SO_2 electrolysis, *Int. J. Hydrogen Energy*, 2012, **37**, 603–614.

32 M. Kanezashi, K. Yada, T. Yoshioka and T. Tsuru, Design of silica networks for development of highly permeable hydrogen separation membranes with hydrothermal stability, *J. Am. Chem. Soc.*, 2009, **131**, 414–415.

33 X. Yu, H. Nagasawa, M. Kanezashi and T. Tsuru, Improved thermal and oxidation stability of bis(triethoxysilyl)ethane (BTESE)-derived membranes, and their gas-permeation properties, *J. Mater. Chem. A*, 2018, **6**, 23378–23387.

34 H. L. Castricum, A. Sah, R. Kreiter, D. H. A. Blank, J. F. Vente and J. E. Ten Elshof, Hydrothermally stable molecular separation membranes from organically linked silica, *J. Mater. Chem.*, 2008, **18**, 2150–2158.

35 W. Puthai, M. Kanezashi, H. Nagasawa, K. Wakamura, H. Ohnishi and T. Tsuru, Effect of firing temperature on the water permeability of SiO_2–ZrO_2 membranes for nanofiltration, *J. Membr. Sci.*, 2016, **497**, 348–356.

36 J. Zhang, R. Zhang, X. Chen, M. Tong, W. Kang, S. Guo, Y. Zhou and J. Lu, Simultaneous Removal of NO and SO_2 from Flue Gas by Ozone Oxidation and NaOH Absorption, *Ind. Eng. Chem. Res.*, 2014, **53**, 6450–6456.

37 L. Meng, M. Kanezashi, J. Wang and T. Tsuru, Permeation properties of BTESE–TEOS organosilica membranes and application to O_2/SO_2 gas separation, *J. Membr. Sci.*, 2015, **496**, 211–218.

38 A. Nadar, A. M. Banerjee, M. Pai, R. Pai, S. S. Meena, R. Tewari and A. Tripathi, Catalytic properties of dispersed iron oxides Fe_2O_3/MO_2 (M= Zr, Ce, Ti and Si) for sulfuric acid decomposition reaction: role of support, *Int. J. Hydrogen Energy*, 2018, **43**, 37–52.

39 M. Landau, S. Varkey, M. Herskowitz, O. Regev, S. Pevzner, T. Sen and Z. Luz, Wetting stability of Si-MCM-41 mesoporous material in neutral, acidic and basic aqueous solutions, *Microporous Mesoporous Mater.*, 1999, **33**, 149–163.

40 H. Nayebzadeh, N. Saghatoleslami and M. Tabasizadeh, Application of microwave irradiation for fabrication of sulfated ZrO_2–Al_2O_3 nanocomposite via combustion method for esterification reaction: process condition evaluation, *J. Nanostruct. Chem.*, 2019, **9**, 141–152.

41 M. Testa, V. La Parola, F. Mesrar, F. Ouanji, M. Kacimi, M. Ziyad and L. Liotta, Use of Zirconium Phosphate-Sulphate as Acid Catalyst for Synthesis of Glycerol-Based Fuel Additives, *Catalysts*, 2019, **9**, 148.

42 P. Graf, D. De Vlieger, B. Mojet and L. Lefferts, New insights in reactivity of hydroxyl groups in water gas shift reaction on Pt/ZrO_2, *J. Catal.*, 2009, **262**, 181–187.

43 T. Ishikawa, Y. Kohtoku, K. Kumagawa, T. Yamamura and T. Nagasawa, High-strength alkali-resistant sintered SiC fibre stable to 2,200 °C, *Nature*, 1998, **391**, 773–775.

44 S. Tomar, S. Gangwar, K. Kondamudi and S. Upadhyayula, SO_3 decomposition over β-SiC and SiO_2 supported $CuFe_2O_4$: a stability and kinetic study, *Int. J. Hydrogen Energy*, 2020, **45**, 21287–21296.

45 H. A. Khan, P. Natarajan and K.-D. Jung, Stabilization of Pt at the inner wall of hollow spherical SiO_2 generated from Pt/hollow spherical SiC for sulfuric acid decomposition, *Appl. Catal., B*, 2018, **231**, 151–160.

46 T. Yoshioka, M. Kanezashi and T. Tsuru, Micropore size estimation on gas separation membranes: a study in experimental and molecular dynamics, *AIChE J.*, 2013, **59**, 2179–2194.

